Integrated random pulse process with positive and negative periodicity

A. V. Kargovsky* and O. A. Chichigina

Faculty of Physics and International Laser Center, Lomonosov Moscow State University, Leninskie Gory, 119991 Moscow, Russia

(Received 21 April 2022; accepted 14 July 2022; published 1 August 2022)

A study of nonstationary processes that are integrals of stationary random sequences of delta pulses is presented. An integrated renewal process can be represented as the sum of a deterministic linear function of time and a Wiener process of the corresponding intensity. This intensity is determined by the mean value and variance of the waiting times of the pulse process and is greater for super-Poisson processes than for sub-Poisson ones. Linear growth over time of all cumulants is proved. An integrated random process with fixed time intervals can be replaced by the sum of a deterministic linear function and a random process with bounded variance. The analytical results are in good agreement with the numerical ones.

DOI: 10.1103/PhysRevE.106.024103

I. INTRODUCTION

The effect of random pulse processes on the dynamic properties of natural, social, and economic systems is of unflagging interest [1–6]. There are two widely used models of pulse processes: renewal pulse processes (RPP) and pulse processes with fixed time intervals (PPFTI). All these processes are characterized by the probability density functions (PDFs) of the times of the appearance of each pulse. If the process is stationary, waiting times (WTs) between two neighboring pulses are identically distributed. In many cases, not only the pulse sequence itself is of interest, but also its integral. Such integrated pulse process is also called the counting process [3,4,7].

When the variance of waiting times is larger than for a Poisson process with the same mean value, the pulse process has super-Poisson statistics [8,9]. Otherwise, the process is sub-Poisson (or quasiperiodic).

The most well-known example of the integrating of the pulse process is registration of the interacting particles [10–12] or photons of the squeezed states of light [13] with the help of a counter or detector. These particles are emitted randomly or quasiperiodically; they are disturbed by the environment, through which they propagated, and interact with each other. All this determines the statistics of the pulse process of particle registration. Counter properties also affect this statistics, for example, a dead time after the registration of each particle.

Another important area of application of these processes is microbiology. The integrated pulse process characterizes the number of particles arrived into a living cell. These particles can be viruses, bacteria, allergens, or, conversely, drug particles and biomarkers [14,15]. The model can also be applied to describe the adhesion of specific viral proteins and their complexes that cause high contagiousness of the current coronavirus infection on surfaces [16].

The renewal pulse process is characterized by independent identically distributed WTs. The PDF of WTs is the only basic characteristic needed to define the process. The renewal process describes a sequence of recurrent events, whose effect is to reset to zero the system's memory [1,2,5,17–20]. A renewal process has asymptotic properties analogous to the strong law of large numbers and the central limit theorem. In addition to the registration of particles, RPP can be used to simulate collisions of billiard particles with the boundary [21–24], moments of resetting in a search process [25–28], earthquakes [29], signals in a neural network [30], the dynamics of animal population [31–36], networks of queues [37], and even crucial events in music [38]. In epidemiology, they describe the statistics of the appearance of new infection cases, including highly infectious diseases such as COVID-19 [35,39].

The pulse process with fixed time intervals is a sequence of pulses appearing in periodic moments with random deviation. Thus, the pulse process is characterized by the probability distribution of deviations [17,19]. PPFTI can model the random process connected with a strongly periodic process, for example, seasonal events regulated by the astronomic year [40,41], scheduled traffic [42], or outbreaks in populations connected with sunspots [43]. They also describe the registration of particles emitted periodically and disturbed by the environment.

The integrated pulse processes are interesting from a theoretical point of view since these pulse processes can be used as a noise source in stochastic differential equations (SDEs) [17,19,32]. The Fokker-Planck formalism for SDE analysis with Gaussian δ-correlated noise is well developed [44]. Meanwhile, pulse noise with nonzero correlation time is a more realistic model of random processes in nature and society [19,34,45,46].

In this paper, we study the possibility of representing random pulse processes as the sum of a regular function and a Gaussian δ-correlated noise. We determine the conditions of application of the methods developed for Gaussian δ-correlated noise to RPP and PPFTI. Such conditions may be

*kargovsky@yumr.phys.msu.ru

defined using the periodicity parameter. It was introduced in Ref. [24] for RPP, and here we generalize the concept of the periodicity parameter to a wider class of random processes.

II. INTEGRATED PULSE PROCESS

Let us consider the point random process,

$$\xi(t) = f_0 \sum_j \delta(t - t_j), \tag{1}$$

consisting of δ-shape pulses with constant positive amplitude f_0. Here, t_j, which is a random variable, represents the time of the jth pulse appearance. This process is characterized by the PDFs $w_m(t)$ of the time t of the appearance of the mth pulse. For a stationary process, $w_m(t)$ is also the PDF that the $(j+m)$-th pulse occurred at t, with t being a time interval calculated starting from the occurrence of the jth pulse.

The waiting times between two neighboring pulses, $\vartheta_j = t_j - t_{j-1}$, are random variables. The spectral density of the stationary stochastic process is equal to the Fourier transform of autocorrelation function $R_{\xi\xi}(\tau)$ (Wiener-Khinchin theorem),

$$S(\omega) = \int_{-\infty}^{\infty} R_{\xi\xi}(\tau) e^{-i\omega\tau} d\tau. \tag{2}$$

Note that some authors [1,47] use a factor of two in this expression.

We use a periodicity parameter in the following form:

$$\rho = 1 - \langle\vartheta\rangle \frac{S(0)}{f_0^2}. \tag{3}$$

This parameter turns to one for strongly sub-Poisson processes, equals zero for the Poisson process, and takes on negative values for super-Poisson processes, which can therefore be assigned to a negative periodicity. Below we restrict ourselves to consider the case of a unit amplitude $f_0 = 1$ only.

Another important characteristic of the pulse process is the correlation time, which is zero for a Poisson process and becomes large for strongly sub- and super-Poisson processes [19,31,35].

The equation for the number of pulses arrived at the time t is

$$m(t) = \int_0^t \xi(t')dt'. \tag{4}$$

We consider the simplest SDE (4) here; meanwhile, any SDE can be represented in such a way that the derivative of the main parameter is defined by deterministic term and noise. Therefore, the properties of the integrated process determine the solution.

The integral of the pulse process is the number of pulses. Let $P_m(t)$ be the probability that there are exactly m pulses at the time t. This probability can be represented as

$$P_m(t) = P_{\geqslant m}(t) P_{<m+1/\geqslant m}(t), \tag{5}$$

where $P_{\geqslant m}(t)$ is the probability that the number of pulses is greater than or equal to m at the time t and $P_{<m+1/\geqslant m}(t)$ is the conditional probability that the number of pulses is less than $m+1$ if this number is greater than or equal to m:

$$\begin{aligned} P_{<m+1/\geqslant m}(t) &= 1 - P_{\geqslant m+1/\geqslant m}(t) \\ &= 1 - \frac{P_{\geqslant m+1,\geqslant m}(t)}{P_{\geqslant m}(t)} = 1 - \frac{P_{\geqslant m+1}(t)}{P_{\geqslant m}(t)}. \end{aligned} \tag{6}$$

Substituting Eq. (6) into Eq. (5), we get

$$P_m(t) = P_{\geqslant m}(t) - P_{\geqslant m+1}(t). \tag{7}$$

Now calculate the probability of the first pulse appearance as if at the initial time moment was a pulse, and we take into account this zeroth pulse. The event that the number of pulses is greater than m is equivalent to the event that the $(m-1)$-th pulse occurred before t. Thus, for the probability, it holds

$$P_{\geqslant m}(t) = \int_{0^-}^t w_{m-1}(t')dt'. \tag{8}$$

Substituting Eq. (8) into Eq. (7), we obtain

$$P_m(t) = \int_{0^-}^t w_{m-1}(t')dt' - \int_{0^-}^t w_m(t')dt', \tag{9}$$

which coincides with the Poisson distribution if $w_m(t)$ is given by the gamma distribution.

III. RENEWAL PULSE PROCESS

For the renewal pulse process, the waiting times between two neighboring pulses are independent identically distributed random variables. The PDF of the time t of appearance of the mth pulse can be presented in the form

$$w_m(t) = \underbrace{w(t) \otimes \cdots \otimes w(t)}_{m \text{ times}}, \tag{10}$$

where $w(t)$ is the PDF of WTs.

Now consider the moment generating function (MGF),

$$\mathcal{M}(s) = \mathbb{E}[e^{sm}], \quad \mu_n' = \partial_s^n \mathcal{M}(s)|_{s\to 0}, \tag{11}$$

where μ_n' is the nth raw moment of the integrated process. Below we assume $s \geqslant 0$. Substituting Eq. (9) into Eq. (11), we get

$$\begin{aligned} \mathcal{M}(s,t) &= \sum_{m=1} e^{sm} \int_{0^-}^t [w_{m-1}(t') - w_m(t')]dt' \\ &= e^s \int_{0^-}^t w_0(t')dt' + (e^s - 1) \sum_{m=1} e^{sm} \int_{0^-}^t w_m(t')dt'. \end{aligned} \tag{12}$$

Using Eq. (10), the Laplace transform of MGF is written as

$$\begin{aligned} \tilde{\mathcal{M}}(s,p) &\equiv \mathcal{L}[\mathcal{M}(s,t)](p) \\ &= \frac{e^s}{p}\left[1 + (e^s - 1)\tilde{w}(p) \sum_{m=0} e^{sm} \tilde{w}^m(p)\right], \end{aligned} \tag{13}$$

where $\tilde{w}(p)$ is the Laplace transform of the PDF of WTs, $w(t)$. Here the power series converges to $[1 - e^s\tilde{w}(p)]^{-1}$ in $D = \{|\tilde{w}(p)| < e^{-s}\}$. By the analytic continuation of the latter function, the domain D can be extended to a larger subset of the image of $\tilde{w}(p)$, except for the singularity $\tilde{w}(p) = e^{-s}$.

Then we have

$$\tilde{\mathcal{M}}(s,p)=\frac{1-\tilde{w}(p)}{p\,[e^{-s}-\tilde{w}(p)]}. \tag{14}$$

At $s=0$, we have the obvious result $\tilde{\mathcal{M}}(0,p)=p^{-1}$ and $\mathcal{M}(0,t)=1$. Further, consider $s\neq 0$. Point $p=0$ is regular,

$$\lim_{p\to 0}\tilde{\mathcal{M}}(s,p)=\frac{\partial_p\tilde{w}(0)}{1-e^{-s}}, \tag{15}$$

where $\partial_p^n\tilde{w}(p)=\mathcal{L}[(-t)^n w(t)](p)$. Note that $\partial_p^0\tilde{w}(p)=\tilde{w}(p)$, $\tilde{w}(0)=1$, and $\partial_p^n\tilde{w}(0)=(-1)^n\mu'_{n\vartheta}$ $(n\in\mathbb{N})$, where $\mu'_{n\vartheta}$ is the nth raw moment of waiting times.

Assume that $\tilde{w}(p)$ is a meromorphic function. Then the singularities $\{p_\lambda\}$ of $\tilde{w}(p)$ are the removable singularities of $\tilde{\mathcal{M}}(s,p)$ since

$$\lim_{p\to p_\lambda}\tilde{\mathcal{M}}(s,p)=\frac{1}{p_\lambda},\quad p_\lambda\neq 0. \tag{16}$$

Now consider the solutions $\{p_k(s)\}$ of equation

$$\tilde{w}(p)=e^{-s}. \tag{17}$$

Without loss of generality, we number $\{p_k(s)\}$ in descending order of the value of the real part. The function $\tilde{w}(p)$ is continuous along the non-negative real axis. Moreover, it is strictly decreasing because

$$\partial_p\tilde{w}(p)=-\int_0^\infty e^{-pt}\,t\,w(t)dt<0,\quad p\in\mathbb{R}_{\geqslant 0}.$$

Then, for $s\geqslant 0$, at least one real root of Eq. (17), $p_k\geqslant 0$, exists. Show that p_0 is a real number. Let $p_{\mathbb{R}}$ and $p_{\mathbb{C}}$ be the first non-negative real element and the first complex element with nonzero imaginary part and non-negative real part (if such exists) of the sequence $\{p_k\}$, respectively:

$$\max_{\{p_k\}\cap\mathbb{R}}\operatorname{Re}p_k=p_{\mathbb{R}}\geqslant 0,$$

$$\max_{\{p_k\}\setminus\mathbb{R}}\operatorname{Re}p_k=\operatorname{Re}p_{\mathbb{C}}\geqslant 0,\quad \operatorname{Im}p_{\mathbb{C}}\neq 0.$$

Then, we have

$$\operatorname{Im}\int_0^\infty e^{-p_{\mathbb{C}}t}w(t)dt=0,$$

$$\begin{aligned}e^{-s}&=\int_0^\infty e^{-p_{\mathbb{R}}t}w(t)dt\\&=\int_0^\infty e^{-\operatorname{Re}p_{\mathbb{C}}t}\cos(\operatorname{Im}p_{\mathbb{C}}t)w(t)dt\\&<\int_0^\infty e^{-\operatorname{Re}p_{\mathbb{C}}t}w(t)dt.\end{aligned}$$

Since $\tilde{w}(p)$ is strictly decreasing, we have $p_{\mathbb{R}}>\operatorname{Re}p_{\mathbb{C}}$ and, consequently, $p_0=p_{\mathbb{R}}$ is a non-negative real number.

Now consider the behavior of expression $e^{-s}-\tilde{w}(p)$ in the neighborhood of the first root p_0 of Eq. (17). Expanding $\tilde{w}(p)$ into the Taylor series, we get

$$\begin{aligned}e^{-s}-\tilde{w}(p)=&-(p-p_0)\\&\times\left[\partial_p\tilde{w}(p_0)+\tfrac{1}{2}\partial_p^2\tilde{w}(p_0)(p-p_0)+\cdots\right].\end{aligned}$$

Since $\partial_p\tilde{w}(p_0)<0$, we conclude that p_0 is a simple root of Eq. (17) and, consequently, a simple pole of $\tilde{\mathcal{M}}(s,p)$, the case of $p_0(0)=0$ was considered above.

If p_k is a simple pole, then

$$\operatorname*{Res}_{p=p_k}e^{pt}\tilde{\mathcal{M}}(s,p)=\frac{e^{p_kt}}{p_k}\frac{\tilde{w}(p_k)-1}{\partial_p\tilde{w}(p_k)}. \tag{18}$$

For higher-order poles, the expression for residue becomes more complicated. Basically, it can be written using the general Leibniz rule and Faà di Bruno's formula, but for our purposes, it is sufficient that it can be presented in the form

$$\operatorname*{Res}_{p=p_k}e^{pt}\tilde{\mathcal{M}}(s,p)=e^{p_kt}\mathscr{P}^{[k]}_{n_k-1}(t), \tag{19}$$

where n_k is the order of the kth pole and $\mathscr{P}^{[k]}_j(t)$ is a polynomial of degree j with the coefficients depending on $\{p_k^{-l}\}_{l=1}^{n_k}$, $\{\partial_p^l\tilde{w}(p_k)\}_{l=0}^{2n_k-1}$. For instance, $\mathscr{P}^{[k]}_0(t)=[\tilde{w}(p_k)-1]/[p_k\,\partial_p\tilde{w}(p_k)]$.

Applying the inverse Laplace transform, we obtain

$$\mathcal{M}(s,t)=\sum_{k=0}e^{p_kt}\mathscr{P}^{[k]}_{n_k-1}(t). \tag{20}$$

Consider the cumulant generating function (CGF) defined as

$$\mathcal{K}(s,t)=\ln\mathcal{M}(s,t),\quad \kappa_n(t)=\partial_s^n\mathcal{K}(s,t)|_{s\to 0}. \tag{21}$$

In the long-time limit, CGF can be sufficiently simplified,

$$\begin{aligned}&\lim_{t\to\infty}\mathcal{K}(s,t)\\&=\lim_{t\to\infty}\ln e^{p_0t}\left[\frac{\tilde{w}(p_0)-1}{p_0\;\partial_p\tilde{w}(p_0)}+\sum_{k=1}e^{-(p_0-p_k)t}\mathscr{P}^{[k]}_{n_k-1}(t)\right]\\&=p_0t,\end{aligned} \tag{22}$$

since the expression in square brackets tends to a constant nonzero first term for at least a finite number of terms in the sum due to the exponential factors with a negative real part of the exponent, and the cumulants become linear:

$$\kappa_n=\partial_s^n p_0(s)|_{s\to 0}\,t. \tag{23}$$

Using Eq. (17), we obtain

$$\partial_s p_0(s)=-\left.\frac{1}{e^s\partial_p\tilde{w}(p)}\right|_{p=p_0(s)},$$

$$\partial_s^2 p_0(s)=-\partial_s p_0(s)-[\partial_s p_0(s)]^2\left.\frac{\partial_p^2\tilde{w}(p)}{\partial_p\tilde{w}(p)}\right|_{p=p_0(s)},$$

and so on. Finally, we get

$$\langle m\rangle=\kappa_1=\frac{t}{\mu'_{1\vartheta}}, \tag{24}$$

$$\sigma_m^2=\kappa_2=\frac{\sigma_\vartheta^2}{\mu'^2_{1\vartheta}}\frac{t}{\mu'_{1\vartheta}}, \tag{25}$$

$$\kappa_3=\left(3\frac{\sigma_\vartheta^4}{\mu'^4_{1\vartheta}}-\frac{\kappa_{3\vartheta}}{\mu'^3_{1\vartheta}}\right)\frac{t}{\mu'_{1\vartheta}}, \tag{26}$$

$$\kappa_4=\left(15\frac{\sigma_\vartheta^6}{\mu'^6_{1\vartheta}}-10\frac{\kappa_{3\vartheta}\sigma_\vartheta^2}{\mu'^5_{1\vartheta}}+\frac{\kappa_{4\vartheta}}{\mu'^4_{1\vartheta}}\right)\frac{t}{\mu'_{1\vartheta}}, \tag{27}$$

$$\kappa_5 = \left(105\frac{\sigma_\vartheta^8}{\mu_{1\vartheta}'^8} - 105\frac{\kappa_{3\vartheta}\sigma_\vartheta^4}{\mu_{1\vartheta}'^7} + 15\frac{\kappa_{4\vartheta}\sigma_\vartheta^2}{\mu_{1\vartheta}'^6} + 10\frac{\kappa_{3\vartheta}^2}{\mu_{1\vartheta}'^6} - \frac{\kappa_{5\vartheta}}{\mu_{1\vartheta}'^5}\right)\frac{t}{\mu_{1\vartheta}'}, \tag{28}$$

$$\kappa_6 = \left(945\frac{\sigma_\vartheta^{10}}{\mu_{1\vartheta}'^{10}} - 1260\frac{\kappa_{3\vartheta}\sigma_\vartheta^6}{\mu_{1\vartheta}'^9} + 210\frac{\kappa_{4\vartheta}\sigma_\vartheta^4}{\mu_{1\vartheta}'^8} + 280\frac{\kappa_{3\vartheta}^2\sigma_\vartheta^2}{\mu_{1\vartheta}'^8} - 21\frac{\kappa_{5\vartheta}\sigma_\vartheta^2}{\mu_{1\vartheta}'^7} - 35\frac{\kappa_{3\vartheta}\kappa_{4\vartheta}}{\mu_{1\vartheta}'^7} + \frac{\kappa_{6\vartheta}}{\mu_{1\vartheta}'^6}\right)\frac{t}{\mu_{1\vartheta}'}, \tag{29}$$

where $\mu_{1\vartheta}'$, σ_ϑ^2, and $\kappa_{n\vartheta}$ are the mean value, variance, and cumulants of the waiting times, respectively. Formulas (24) and (25) coincide with the expressions obtained in Refs. [2,48]. For the skewness γ_1 and kurtosis excess γ_2, we obtain

$$\gamma_1 = \left(3\frac{\sigma_\vartheta}{\mu_{1\vartheta}'} - \gamma_{1\vartheta}\right)\left(\frac{t}{\mu_{1\vartheta}'}\right)^{-\frac{1}{2}}, \tag{30}$$

$$\gamma_2 = \left(\gamma_{2\vartheta} - 10\frac{\gamma_{1\vartheta}\sigma_\vartheta}{\mu_{1\vartheta}'} + 15\frac{\sigma_\vartheta^2}{\mu_{1\vartheta}'^2}\right)\left(\frac{t}{\mu_{1\vartheta}'}\right)^{-1}. \tag{31}$$

Here, $\gamma_{1\vartheta}$ and $\gamma_{2\vartheta}$ denote the skewness and kurtosis excess of the waiting times, respectively.

Using Eqs. (30) and (31), we can estimate the time it takes for the skewness and kurtosis excess to become small enough to consider the pulse process as Gaussian noise and its integral as a Wiener process,

$$t \gg \tau_W = \mu_{1\vartheta}' \max\left(\left[3\frac{\sigma_\vartheta}{\mu_{1\vartheta}'} - \gamma_{1\vartheta}\right]^2, \gamma_{2\vartheta} - 10\frac{\gamma_{1\vartheta}\sigma_\vartheta}{\mu_{1\vartheta}'} + 15\frac{\sigma_\vartheta^2}{\mu_{1\vartheta}'^2}\right). \tag{32}$$

The above consideration was based on the assumption that the function $\tilde{w}(p)$ has no branch points. The case of multivalued functions requires more detailed analysis. Let us consider that no branch point of $\tilde{w}(p)$ coincides with the root p_0. Assume the branch cuts $\mathcal{C}$ of $\tilde{w}(p)$ can be chosen in such a way that they stay left from the Bromwich integral path. To apply the residue theorem to calculate the Bromwich integral, the contour must be closed in accordance with such branch cuts, i.e., the contour should not cross the branch cuts (see Fig. 1, for example). This leads to the appearance of additional terms in Eq. (20). Let us estimate them in the long-time limit. First, note that for large p, the function $\tilde{\mathcal{M}}(s,p)$ behaves as p^{-1}. Consequently, the contributions along the large arcs vanish as their radius tends to infinity according to Jordan's lemma [49]. The integral around the branch point, $p_{\text{b.p.}}$ (if it is not the zero of the denominator of Eq. (14) or, otherwise, if $\tilde{\mathcal{M}}(s,p) \sim (p - p_{\text{b.p.}})^\sigma$ with $\operatorname{Re}\sigma > -1$ in some neighborhood of the branch point), can be shown to contribute nothing as the radius of the small arc goes to zero. The integrals along the branch cut give the contribution

$$\Delta = \frac{e^{p_{\text{b.p.}}t}}{2\pi i}\int_0^\infty e^{-\zeta t}\phi(\zeta)d\zeta,$$
$$\phi(\zeta) = \tilde{\mathcal{M}}(s, e^{-i\pi}\zeta + p_{\text{b.p.}}) - \tilde{\mathcal{M}}(s, e^{i\pi}\zeta + p_{\text{b.p.}}). \tag{33}$$

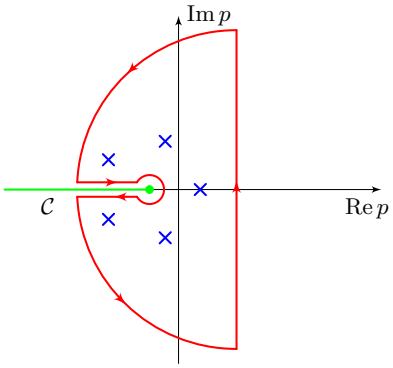

FIG. 1. Sample contour for evaluating the Bromwich integral.

In general, $|\tilde{\mathcal{M}}(s,p)|$ is bounded along the branch cut; however, there may be some exceptions corresponding to the poles of $\tilde{\mathcal{M}}(s,p)$ that lie on the branch cut. If such poles are simple, then the principal values of the integrals (33) are well defined or we can change the branch cut in a certain way. Further, if $\phi(\zeta)$ is of the form $\phi(\zeta) = \zeta^\sigma g(\zeta)$, where $\operatorname{Re}\sigma > -1$, $g(0) \neq 0$, and $g(\zeta)$ is continuous in some neighborhood of $\zeta = 0$, the Watson's lemma [50] conditions are satisfied and we obtain

$$\Delta = \frac{e^{p_{\text{b.p.}}t}}{2\pi i}\left[\frac{g(0)\Gamma(\sigma+1)}{t^{\sigma+1}} + o(t^{-\sigma-1})\right], \quad t \to \infty. \tag{34}$$

Similar exponential estimations can be obtained for some other kinds of branch cuts. Finally, we get that for $\operatorname{Re} p_{\text{b.p.}} < p_0$, formulas (24)–(29) remain valid in the long-time limit.

A. Probability per unit of time for pulse appearance and PDF of WTs

Let the probability per unit of time for pulse appearance be $p(t)$. Discrete time is written as $t_m = m\Delta t$, where Δt is the time step. The probability of pulse appearing at the mth step is equal to $p(t_m)\Delta t$. The probability that the waiting time is equal to m steps can be presented in the form

$$P_m = p(t_{m+1})\Delta t \prod_{k=1}^{m}[1 - p(t_k)\Delta t] = p(t_{m+1})\Delta t \exp\left(\sum_{k=1}^{m}\ln[1 - p(t_k)\Delta t]\right).$$

In the limit of small Δt, we change the sum to an integral and obtain the PDF of WTs,

$$w(\vartheta) = p(\vartheta)\exp\left[-\int_0^\vartheta p(t)dt\right]. \tag{35}$$

The inversion formula is easy obtained as

$$p(t) = w(t)\left[\int_t^\infty w(\vartheta)d\vartheta\right]^{-1}. \tag{36}$$

B. Examples of RPP with different distributions of WTs

Let us consider the point renewal process (1). The distribution of waiting times can be shifted with shift parameter

TABLE I. Characteristics of used distributions of waiting times for RPP.

	Shifted gamma distribution Eq. (37)	Shifted Weibull distribution Eq. (38)[a]	Pareto distribution Eq. (39)[b]
$\langle\vartheta\rangle$	$\alpha n+\vartheta_0$	$\alpha\,\Gamma_1+\vartheta_0$	$\frac{n\vartheta_0}{n-1}$
σ^2_ϑ	$\alpha^2 n$	$\alpha^2(\Gamma_2-\Gamma_1^2)$	$\frac{n}{n-2}(\frac{\vartheta_0}{n-1})^2$
$\kappa_{3\vartheta}$	$2\alpha^3 n$	$\alpha^3(\Gamma_3-3\Gamma_2\Gamma_1+2\Gamma_1^3)$	$\frac{2n(n+1)}{(n-2)(n-3)}(\frac{\vartheta_0}{n-1})^3$
$\kappa_{4\vartheta}$	$6\alpha^4 n$	$\alpha^4(\Gamma_4-4\Gamma_3\Gamma_1-3\Gamma_2^2+12\Gamma_2\Gamma_1^2-6\Gamma_1^4)$	$\frac{6n(n^3+n^2-6n-2)}{(n-2)^2(n-3)(n-4)}(\frac{\vartheta_0}{n-1})^4$
$1-\rho$	$\frac{\alpha^2 n}{(\alpha n+\vartheta_0)^2}$	$\frac{\alpha^2(\Gamma_2-\Gamma_1^2)}{(\alpha\Gamma_1+\vartheta_0)^2}$	$\frac{1}{n(n-2)}$
$p(t),\times\mathbb{1}_{t\geqslant\vartheta_0}$	$\frac{(t-\vartheta_0)^{n-1}}{\Gamma(n,\frac{t-\vartheta_0}{\alpha})\alpha^n}\exp(-\frac{t-\vartheta_0}{\alpha})$	$\frac{n(t-\vartheta_0)^{n-1}}{\alpha^n}$	$\frac{n}{t}$

[a]Use notation $\Gamma_j\equiv\Gamma(1+j/n)$.

[b]Note that the moments and the cumulant of order j are defined for $n>j$ only.

ϑ_0 and $\vartheta\in[\vartheta_0,\infty)$. Below, n and α are the shape and scale parameters, respectively. The processes are periodical at $n\to\infty$.

(i) Shifted gamma distribution [35,51,52]:

$$w(\vartheta)=\frac{(\vartheta-\vartheta_0)^{n-1}}{\Gamma(n)\alpha^n}\,\exp\left(-\frac{\vartheta-\vartheta_0}{\alpha}\right)\mathbb{1}_{\vartheta\geqslant\vartheta_0}. \tag{37}$$

In the case of Poisson statistics ($n=1$, $\vartheta_0=0$), we get δ correlation.

(ii) Shifted Weibull distribution:

$$w(\vartheta)=\frac{n}{\alpha}\left(\frac{\vartheta-\vartheta_0}{\alpha}\right)^{n-1}\times\exp\left(-\left[\frac{\vartheta-\vartheta_0}{\alpha}\right]^n\right)\mathbb{1}_{\vartheta\geqslant\vartheta_0},\quad n>0. \tag{38}$$

The Poisson statistics is realized for $n=1$ and $\vartheta_0=0$.

(iii) Pareto distribution:

$$w(\vartheta)=\frac{n\vartheta_0^n}{\vartheta^{n+1}}\,\mathbb{1}_{\vartheta\geqslant\vartheta_0},\quad n>2, \tag{39}$$

where ϑ_0 plays the role of the shift and scale parameters simultaneously. The process is super-Poisson for $2<n<1+\sqrt{2}$ and sub-Poisson for $n>1+\sqrt{2}$. Some high-order moments do not exist for this distribution. If n is not an integer, the Laplace transform of Eq. (39) has a branch point at the origin and therefore the root p_0 of Eq. (17) is not an isolated singularity at $s\to 0$. This case requires separate consideration (see the Appendix).

Some properties of these distributions are collected in Table I.

IV. PULSE PROCESS WITH FIXED TIME INTERVALS

In the case of the pulse process with fixed time intervals, the time of the $(m+1)$-th pulse appearance is $t_{m+1}=Tm+\nu$, where $-T/2<\nu<T/2$ is a random deviation, characterized by the PDF $w(\nu)$. The corresponding probabilities of the pulse number can be written as

$$P_{\geqslant m}(t)=1-\mathbb{1}_{m>1}\int_{t-(m-1)T}^{\frac{T}{2}}w(\nu)d\nu, \tag{40}$$

$$P_m(t)=\int_{t-mT}^{t^*}w(\nu)d\nu,$$

$$t^*=t-(m-1)T+\delta_{m1}\left(\frac{T}{2}-t\right). \tag{41}$$

Below, in this section, the square and curly brackets denote the integer and fractional part of a real number, respectively. The equation for the number of pulses arrived at the time t [see Eq. (4)] is

$$m(t)=\mathbb{1}_{t<T/2}+\left[\frac{t}{T}+\frac{1}{2}\right]+\beta(t), \tag{42}$$

where $\beta(t)\sim\mathrm{Bern}[P_{+1}(t)]$ is a Bernoulli distributed random variable. Here, $P_{+1}(t)$ is the probability of the appearance of one more pulse, which is a periodical function,

$$P_{+1}(t)=\mathbb{1}_{t\geqslant T/2}\int_{-\frac{T}{2}}^{T\left\{\frac{t}{T}+\frac{1}{2}\right\}-\frac{T}{2}}w(\nu)d\nu. \tag{43}$$

Note that the integrated process can be presented as a deterministic step increasing part and bounded random process. Using Eq. (42), we get

$$\langle m\rangle=\mathbb{1}_{t<T/2}+\left[\frac{t}{T}+\frac{1}{2}\right]+P_{+1}(t). \tag{44}$$

It is easy to see that for $t\geqslant T/2$, Eq. (44) can be presented as the sum of a linear increasing and oscillating functions.

Other statistical properties of the process are determined by the Bernoulli distribution with the periodic probability $P_{+1}(t)$. The variance is

$$\sigma_m^2=P_{+1}(t)-P_{+1}^2(t), \tag{45}$$

which is a periodic function of time also. It is known [17] that the correlation time is infinite and $S(0)=0$ for PPFTI.

For the cumulants, we have

$$\kappa_3=2P_{+1}^3(t)-3P_{+1}^2(t)+P_{+1}(t), \tag{46}$$

$$\kappa_4=-6P_{+1}^4(t)+12P_{+1}^3(t)-7P_{+1}^2(t)+P_{+1}(t). \tag{47}$$

This process does not become Gaussian. Meanwhile, we can see another kind of simplification for PPFTI as an opportunity to neglect by the random part of the process since it does not increase with time. This part can be called zero-intensity white noise.

TABLE II. Characteristics of used distributions of deviations for PPFTI.

	Uniform distribution Eq. (48)	Localized distribution Eq. (50)
$w(\vartheta)$	$\frac{\alpha-\lvert\vartheta-T\rvert}{\alpha^2}\mathbb{1}_{\lvert\vartheta-T\rvert\leqslant\alpha}$	$\sum_{l=-1}^{1}\frac{1}{2^{\lvert l\rvert+1}}\delta(\vartheta-T+l\alpha)$
$\langle\vartheta\rangle$	T	T
σ_ϑ^2	$\frac{\alpha^2}{6}$	$\frac{\alpha^2}{2}$
$P_{+1}(t),\ \times\mathbb{1}_{t\geqslant T/2}$	$\max\left[0,\ \min\left(\frac{T}{\alpha}\left\{\frac{t}{T}+\frac{1}{2}\right\}-\frac{T-\alpha}{2\alpha},\ 1\right)\right]$	$\frac{1}{2}\sum_{l=0}^{1}\mathbb{1}_{\left\{\frac{t}{T}+\frac{1}{2}\right\}>\frac{T+(-1)^l\alpha}{2T}}$

Examples of PPFTI with different distributions of deviations

(i) Uniform distribution:

$$w(\nu)=\frac{1}{\alpha},\quad \alpha\leqslant T,\quad |\nu|<\frac{\alpha}{2}. \tag{48}$$

The maximum variance corresponds to $\alpha=T$ and the mean value (44) can be written in a simple form,

$$\langle m\rangle=1+\left(\frac{t}{T}-\frac{1}{2}\right)\mathbb{1}_{t\geqslant T/2}. \tag{49}$$

(ii) Localized distribution:

$$w(\nu)=\frac{1}{2}\delta\left(\nu-\frac{\alpha}{2}\right)+\frac{1}{2}\delta\left(\nu+\frac{\alpha}{2}\right),\quad \alpha<T. \tag{50}$$

This process can reach larger variances than the process with the uniform PDF at the same T.

Meanwhile, all PPFTI are sub-Poisson. The corresponding PDF of WTs and other properties of these distributions are collected in Table II.

V. RESULTS AND DISCUSSION

In this section, we present the results obtained by numerical simulations for the integrated random pulse process. The Mersenne twister [53] is used as a pseudorandom number generator. The numerical results are averaged over 10^9 realizations. The period, or mean waiting time, is $\langle\vartheta\rangle=1$.

The time dependence of the mean value (24) and variance (25) for RPP with super-Poisson statistics ($\sigma_\vartheta^2=2$) and various distributions of waiting times are presented in Figs. 2(a) and 2(b). Here, we use the following sets of parameter values: $n=0.5$, $\vartheta_0=0$, and $\alpha=2$ for shifted gamma distribution; $n=0.5$, $\alpha=0.315$, and $\vartheta_0=0.37$ for shifted Weibull distribution; $n=2.22$ and $\vartheta_0=0.55$ for Pareto distribution. Here and below, the lines and symbols represent the analytical and numerical results, respectively. The mean value and variance exhibit near-linear growth over time. The numerical and analytical data are in good agreement. Since, here, $n<3$ for the Pareto distribution, one can see the difference in the time dependence of the variance compared to the shifted gamma and Weibull distributions in the presented time range, which is fully consistent with Eq. (A3).

We have shown that the third (26) and fourth (27) cumulants also increase linearly in time. Figure 3(a) illustrates this dependence for the gamma distribution with $n=0.5$ and $\vartheta_0=0$. The skewness γ_1 (30) and kurtosis excess γ_2 (31) are presented in Fig. 3(b). The number or realizations is increased here to 2×10^{10} due to the large variance.

The time dependence of the mean value (24) and variance (25) for RPP with sub-Poisson statistics ($\sigma_\vartheta^2=0.032$) and various distributions of waiting times are presented in Figs. 4(a)

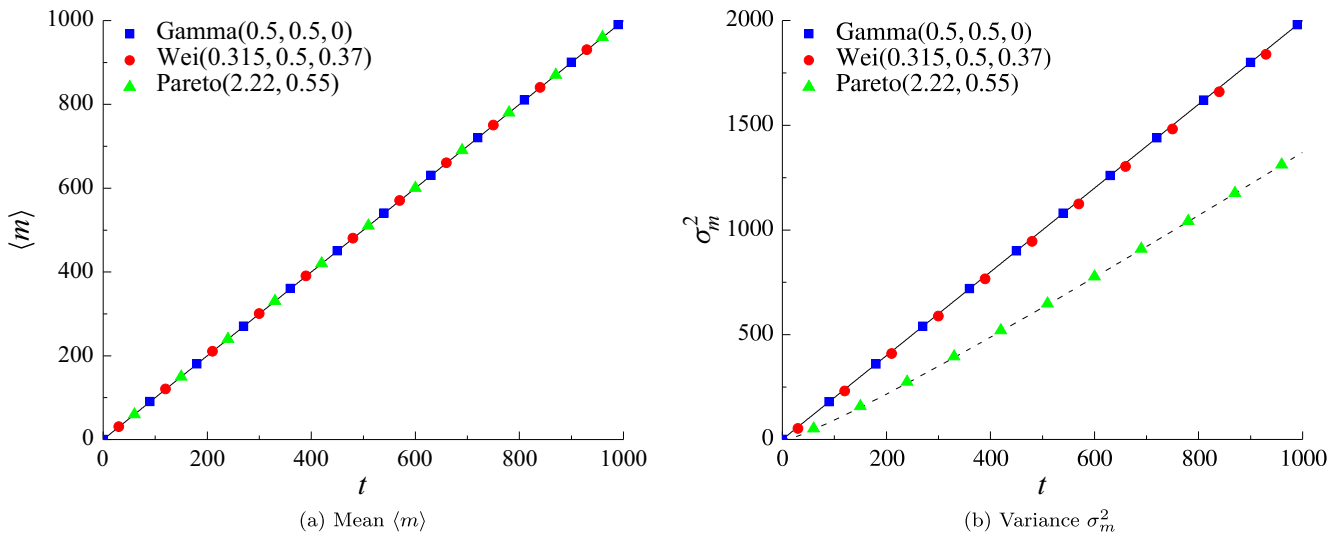

(a) Mean $\langle m\rangle$ (b) Variance σ_m^2

FIG. 2. Plot of mean value and variance of pulse number vs time for RPP with super-Poisson statistics with different distributions of waiting times ($\langle\vartheta\rangle=1$, $\sigma_\vartheta^2=2$): shifted gamma distribution with $n=0.5$, $\alpha=2$, and $\vartheta_0=0$ (blue squares); shifted Weibull distribution with $n=0.5$, $\alpha=0.315$, and $\vartheta_0=0.37$ (red circles); Pareto distribution with $n=2.22$ and $\vartheta_0=0.55$ (green triangles). Analytical solution, obtained from (a) Eq. (24) (solid black line) and (b) Eq. (25) (solid black line), Eq. (A3) (dashed black line).

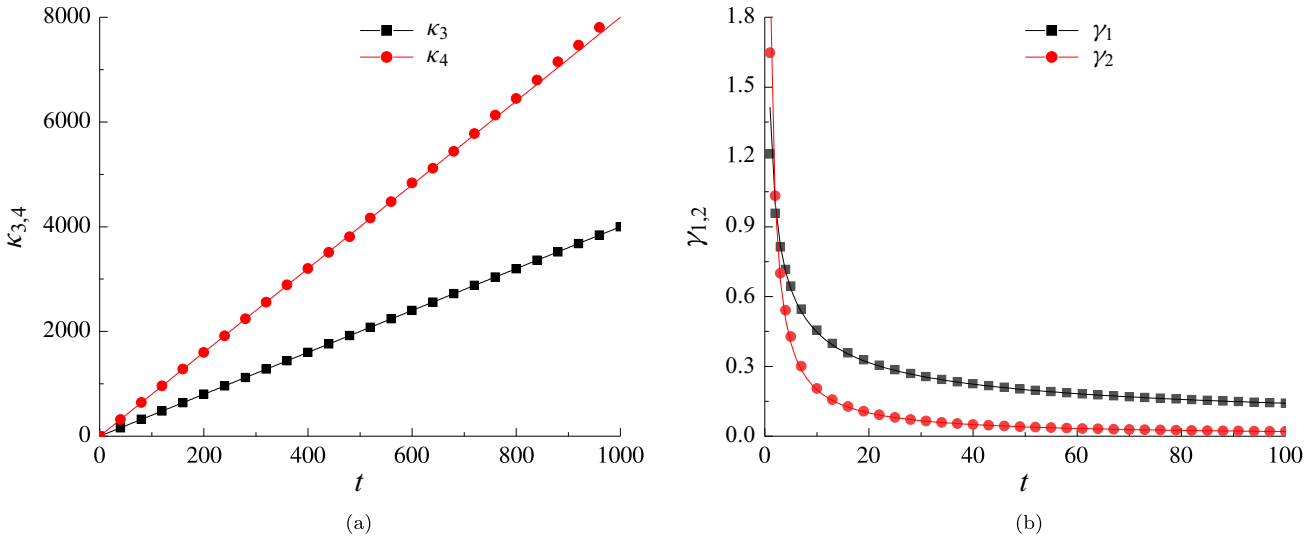

FIG. 3. Plot of higher cumulants and measures of shape of pulse number vs time for RPP with super-Poisson statistics and shifted gamma distribution of waiting times with $n = 0.5$, $\alpha = 2$, and $\vartheta_0 = 0$. (a) Cumulants: κ_3 (black squares), κ_4 (red circles). Analytical solutions, obtained from Eq. (26) (solid black line) and Eq. (27) (solid red line). (b) Skewness γ_1 (black squares) and kurtosis excess γ_2 (red circles). Analytical solutions, obtained from Eq. (30) (solid black line) and Eq. (31) (solid red line).

and 4(b). The following sets of parameter values are used: $n = 20$, $\vartheta_0 = 0.2$, and $\alpha = 0.04$ for shifted gamma distribution; $n = 2$, $\alpha = 0.384$, and $\vartheta_0 = 0.66$ for shifted Weibull distribution; $n = 6.67$ and $\vartheta_0 = 0.85$ for Pareto distribution. We have also added results here for a shifted gamma distribution with the same variance and different parameters $n = 0.2$, $\vartheta_0 = 0.92$, and $\alpha = 0.4$. All these probability density functions are collected in Fig. 5. We can see that they are significantly different from each other. Interestingly, there is a good agreement between the results for the Pareto statistics and other distributions of WTs. Therefore, the sub-Poissonity of the process is a sufficient condition to consider it as a white noise.

The time dependence of the mean value (44) and variance (45) for PPFTI with uniform ($T = 1$, $\alpha = 1$) and localized ($T = 1$, $\alpha = 1/\sqrt{3}$) distributions of deviations are presented in Figs. 6(a) and 6(b). The numerical results are in good agreement with the analytical ones. The condition of $S(0) = 0$ is sufficient to consider this process as white noise for the integrated process, while the correlation time is infinite.

The asymptotic properties of the counting process have been well investigated for $t \to \infty$; meanwhile, for practical purposes, it is important to estimate the finite time after which these properties can be used.

The two conventional conditions for presenting a random process as a Gaussian δ-correlated noise source in SDE are

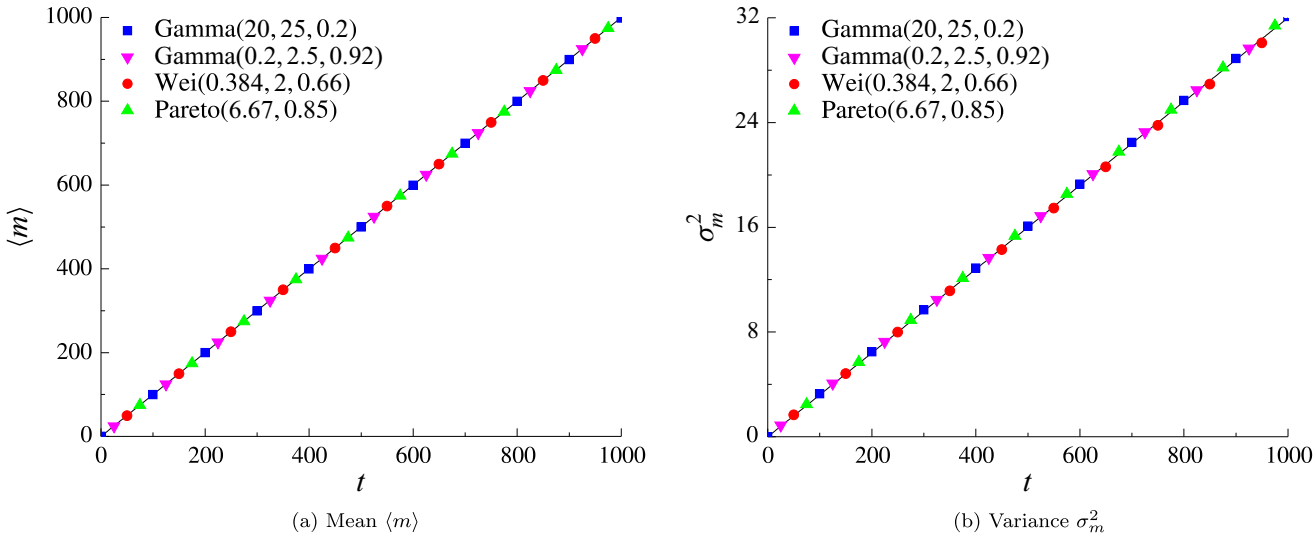

FIG. 4. Plot of mean value and variance of pulse number vs time for RPP with sub-Poisson statistics and different distributions of waiting times ($\langle \vartheta \rangle = 1$, $\sigma_\vartheta^2 = 0.032$): shifted gamma distribution with $n = 20$, $\alpha = 0.04$, and $\vartheta_0 = 0.2$ (blue squares); shifted gamma distribution with $n = 0.2$, $\alpha = 0.4$, and $\vartheta_0 = 0.92$ (magenta down triangles); shifted Weibull distribution with $n = 2$, $\alpha = 0.384$, and $\vartheta_0 = 0.66$ (red circles); Pareto distribution with $n = 6.67$ and $\vartheta_0 = 0.85$ (green up triangles). Analytical solution, obtained from (a) Eq. (24) and (b) Eq. (25) (solid black lines).

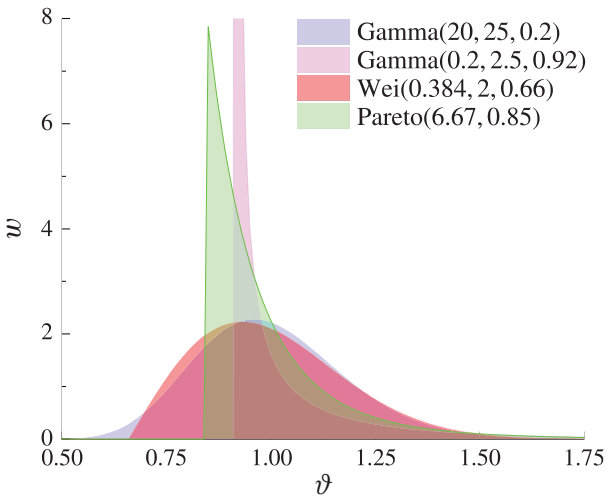

FIG. 5. Probability density functions of waiting times for sub-Poisson process ($\langle\vartheta\rangle = 1$, $\sigma_\vartheta^2 = 0.032$): shifted gamma distribution with $n = 20$, $\alpha = 0.04$, and $\vartheta_0 = 0.2$ (blue); shifted gamma distribution with $n = 0.2$, $\alpha = 0.4$, and $\vartheta_0 = 0.92$ (magenta); shifted Weibull distribution with $n = 2$, $\alpha = 0.384$, and $\vartheta_0 = 0.66$ (red); Pareto distribution with $n = 6.67$ and $\vartheta_0 = 0.85$ (green).

that (i) its intensity is much less than the characteristic scale of the process and (ii) the correlation time is much less than the characteristic timescale of the process. We define new conditions for such a replacement.

We can see that the key characteristic is $S(0)/f_0^2$, which is greater than $\langle\vartheta\rangle^{-1}$ for super-Poisson processes and less for the sub-Poisson. This parameter should be small enough for the simplification. As a result, the correlation time does not determine the possibility of the simplification. This time is long for strongly sub-Poisson processes and infinite for PPFTI, but these processes arrive at a simplified model after several periods. The characteristic time determined by Eq. (32) is also greater for super-Poisson than for sub-Poisson processes.

For example, in the case of the gamma distribution of WTs, it is equal to $\sigma_\vartheta^2/\mu'_{1\vartheta}$. We can also say that the greater the periodicity ρ, the better the asymptotic simplifications work. Therefore, the strongly super-Poisson processes are the most complicated for calculations and special simplification methods are needed [24]. Meanwhile, for all other processes, we can see good agreement of the numerical simulations with the results obtained using asymptotically simplified models.

This point represents the main topic of our work since it is now possible to give a quantitative definition of the pulse process, the integral of which can be considered as the integral of white noise. The results obtained here by using several specific PDFs of WTs can be generalized to other distributions.

ACKNOWLEDGMENTS

This work was supported by the Russian Foundation for Basic Research, Grant No. 20-04-60505. The authors are thankful to Professor A. Dubkov for useful suggestions on cumulant analysis and to Professor N. Brandt for fruitful discussions. The research is carried out using the equipment of the shared research facilities of HPC computing resources at Lomonosov Moscow State University [54].

APPENDIX: CUMULANTS OF RPP WITH PARETO DISTRIBUTION OF WTs WITH NONINTEGER *n*

The Laplace transform of Pareto PDF (39) can be written as [55]

$$\tilde{w}(p) = n(p\vartheta_0)^n \Gamma(-n, p\vartheta_0). \tag{A1}$$

Equation (17) has one non-negative real root p_0 and infinite number of complex roots located symmetrically with respect to the real axis. The real parts of all complex roots became negative with $s \to 0$, while the real root tends to zero (see Fig. 7; increasing the size of the markers illustrates the shift of the given root to the left with decrease in s). Also, the origin is

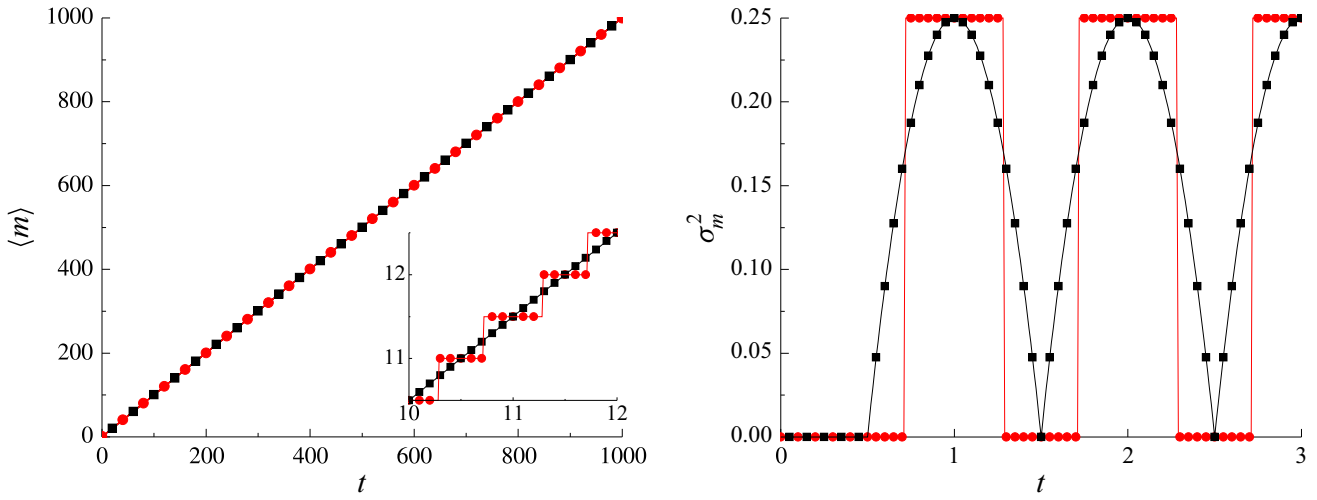

(a) Mean $\langle m\rangle$ (b) Variance σ_m^2

FIG. 6. Plot of mean value and variance of pulse number vs time for PPFTI with different distributions of deviations ($T = 1$, $\sigma_\vartheta^2 = 1/6$): uniform distribution (48) with $\alpha = 1$ (black squares); localized distribution (50) with $\alpha = 1/\sqrt{3}$ (red circles). Analytical solutions, obtained from (a) Eq. (44) and (b) Eq. (45) (solid black and red lines, respectively).

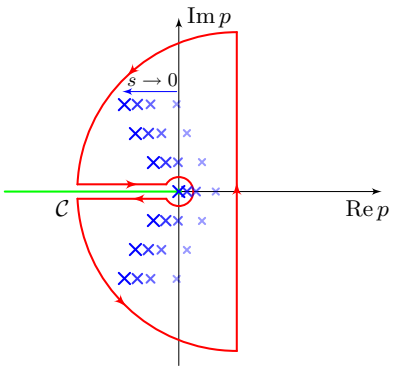

FIG. 7. Contour for evaluating the Bromwich integral for the Pareto PDF of waiting times. Crosses denote the simple poles of $\tilde{\mathcal{M}}(s,p)$; they shift to the left as $s \to 0$.

the branch point of $\tilde{w}(p)$ for noninteger n. Since the condition $\mathrm{Re}\, p_{\mathrm{b.p.}} < p_0$ is violated for $s = 0$, the consideration presented in Sec. III needs to be modified.

Consider the first two cumulants in the long-time limit. Taking into account the obvious relation $\mathcal{M}(0,t) = 1$, we have

$$\langle m \rangle = \kappa_1 = \partial_s \mathcal{M}(s,t)|_{s\to 0},$$
$$\sigma_m^2 = \kappa_2 = \partial_s^2 \mathcal{M}(s,t)|_{s\to 0} - \partial_s \mathcal{M}(s,t)|_{s\to 0}^2.$$

Using Eq. (14) and differentiating the Bromwich integral by parameter s, we get

$$\partial_s \mathcal{M}(s,t)|_{s\to 0} = \frac{1}{2\pi i}\int_{c-i\infty}^{c+i\infty} \frac{e^{pt}}{p}\frac{1}{1-\tilde{w}(p)}dp, \quad c>0,$$

$$\partial_s^2 \mathcal{M}(s,t)|_{s\to 0} = \frac{1}{2\pi i}\int_{c-i\infty}^{c+i\infty} \frac{e^{pt}}{p}\left\{\frac{2}{[1-\tilde{w}(p)]^2} - \frac{1}{1-\tilde{w}(p)}\right\}dp, \quad c>0.$$

In the long-time limit, the main contribution to the integral gives the integral along the branch cut, namely, its part around the origin (the residues at the complex poles contribute negligibly due to the exponential factors with a negative real part of the exponent). Here we use expansion for the incomplete gamma function [55],

$$\Gamma(-n,z) = \Gamma(-n) - \sum_{k=0}^{\infty}\frac{(-1)^k z^{k-n}}{k!(k-n)}, \quad n \notin \mathbb{Z}_{\geqslant 0},$$

and Hankel's loop integral,

$$\frac{1}{\Gamma(\alpha)} = \frac{1}{2\pi i}\int_{-\infty}^{0+} e^z z^{-\alpha} dz, \quad |\arg z| \leqslant \pi,$$

where the contour begins at $-\infty$, circles the origin once in the positive direction and returns to $-\infty$. Expanding the integrand in a power series, we have

$$\begin{aligned}\partial_s \mathcal{M}(s,t)|_{s\to 0} &= \frac{1}{2\pi i}\int_{-\infty}^{0+}\frac{e^{pt}}{p^2}\frac{n-1}{n\vartheta_0} \times\left\{1+(n-1)\Gamma(-n)(p\vartheta_0)^{n-1}+\frac{1}{2}\frac{n-1}{n-2}p\vartheta_0-\cdots\right\}dp\\ &= \frac{t}{\mu'_{1\vartheta}} - \frac{(n-1)\vartheta_0^{n-2}t^{2-n}}{n^2(n-2)} + \frac{(n-1)^2}{2n(n-2)} + O(t^{-1}),\end{aligned}$$

where $\mu'_{1\vartheta} = n\vartheta_0/(n-1)$ according to Table I. Note that we limited our consideration to $n > 2$ [see Eq. (39)], and therefore the second term decreases with time, but we left it here along with the third term for the calculation of the variance below. For the mean value in the long-time limit, we get the same expression as Eq. (24):

$$\langle m \rangle = \frac{t}{\mu'_{1\vartheta}}, \quad n > 2. \tag{A2}$$

Now calculate the variance. In the expression for the second derivative, it suffices to leave the terms giving contributions with positive powers of t. Then we obtain

$$\begin{aligned}\partial_s^2 \mathcal{M}(s,t)|_{s\to 0} &= \frac{1}{2\pi i}\int_{-\infty}^{0+}\frac{e^{pt}}{\mu'_{1\vartheta}p^2}\left\{\frac{2}{\mu'_{1\vartheta}p} + 4\frac{(n-1)^2\Gamma(-n)(p\vartheta_0)^{n-2}}{n} + 2\frac{(n-1)^2}{n(n-2)} - 1 + \cdots\right\}dp\\ &= \left(\frac{t}{\mu'_{1\vartheta}}\right)^2 + \left\{2\frac{(n-1)^2}{n(n-2)} - 1 + 4\frac{(n-1)\vartheta_0^{n-2}t^{2-n}}{n^2(3-n)(2-n)}\right\}\frac{t}{\mu'_{1\vartheta}} + O(1).\end{aligned}$$

Finally, we get

$$\sigma_m^2 = \frac{\sigma_\vartheta^2}{\mu'^2_{1\vartheta}}\frac{t}{\mu'_{1\vartheta}} - 2\frac{\sigma_\vartheta^2}{\mu'^3_{1\vartheta}}\frac{(n-1)^2}{n(3-n)}\vartheta_0^{n-2}t^{3-n}. \tag{A3}$$

Certainly, this expression only makes sense when it is positive. For $n \geqslant 3$, the second term should be omitted and we arrive at the expression (25). If $2 < n < 3$, the second term increases as t^{3-n}, but the linear term will dominate anyway; it just might take much longer to establish Eq. (25).

Corrections for higher cumulants can be obtained in the same way.

[1] R. Stratonovich, *Topics in the Theory of Random Noise* (Gordon and Breach, New York, 1963).
[2] D. R. Cox, *Renewal Theory* (Chapman and Hall, New York, 1967).
[3] J. J. Higgins and S. Keller-McNulty, *Concepts in Probability and Stochastic Modeling* (Duxbury Press, Belmont, 1995).
[4] S. M. Ross, *Stochastic Processes* (Wiley, New York, 1996).
[5] D. J. Daley and D. Vere-Jones, *An Introduction to the Theory of Point Processes* (Springer, New York, 2013).
[6] P. Brémaud, *Point Process Calculus in Time and Space* (Springer, Cham, 2020).

[7] D. Cocco and M. Giona, Generalized counting processes in a stochastic environment, Mathematics **9**, 2573 (2021).

[8] N. Pacilio, T. Ferrari, and P. Lorenzi, A micrologic integrated circuit for monitoring correlation in pulse sequences, Nucl. Instrum. Methods **92**, 13 (1971).

[9] V. S. Beliaeva, O. A. Chichigina, D. S. Klyuev, A. M. Neshcheret, O. V. Osipov, and A. A. Potapov, Semi-phenomenological approach to surface-bonded chiral nanostructures creation based on DNA-origami, in *Advances in Artificial Systems for Medicine and Education III*, edited by Z. Hu, S. Petoukhov, and M. He (Springer, Cham, 2020), pp. 263–272.

[10] N. Y. Agafonova, V. V. Ashikhmin, E. A. Dobrynina, R. I. Enikeev, A. S. Malgin, O. G. Ryazhskaya, I. R. Shakiryanova, and V. F. Yakushev, LVD experiment: 25 years of operation, Phys. Atom. Nuclei **81**, 95 (2018).

[11] N. S. Davis, S. L. Rudge, and D. S. Kosov, Electronic statistics on demand: Bunching, antibunching, positive, and negative correlations in a molecular spin valve, Phys. Rev. B **103**, 205408 (2021).

[12] R. Essick, G. Mo, and E. Katsavounidis, A coincidence null test for Poisson-distributed events, Phys. Rev. D **103**, 042003 (2021).

[13] M. C. Teich and B. E. Saleh, Squeezed state of light, Quantum Opt. **1**, 153 (1989).

[14] K. Galler, K. Bräutigam, C. Große, J. Popp, and U. Neugebauer, Making a big thing of a small cell—Recent advances in single cell analysis, Analyst **139**, 1237 (2014).

[15] Z. Zhai, F. Zhang, X. Chen, J. Zhong, G. Liu, Y. Tian, and Q. Huang, Uptake of silver nanoparticles by DHA-treated cancer cells examined by surface-enhanced Raman spectroscopy in a microfluidic chip, Lab Chip **17**, 1306 (2017).

[16] W. Sungnak, N. Huang, C. Bécavin, M. Berg, R. Queen, M. Litvinukova, C. Talavera-López, H. Maatz, D. Reichart, F. Sampaziotis, K. B. Worlock, M. Yoshida, J. L. Barnes, and HCA Lung Biological Network, SARS-CoV-2 entry factors are highly expressed in nasal epithelial cells together with innate immune genes, Nat. Med. **26**, 681 (2020).

[17] A. V. Kargovsky, O. A. Chichigina, E. I. Anashkina, D. Valenti, and B. Spagnolo, Relaxation dynamics in the presence of pulse multiplicative noise sources with different correlation properties, Phys. Rev. E **92**, 042140 (2015).

[18] D. Valenti, O. Chichigina, A. Dubkov, and B. Spagnolo, Stochastic acceleration in generalized squared Bessel processes, J. Stat. Mech. (2015) P02012.

[19] A. V. Kargovsky, A. Y. Chikishev, and O. A. Chichigina, Effect of multiplicative noise on stationary stochastic process, Phys. Rev. E **97**, 032112 (2018).

[20] W. Wang, J. H. P. Schulz, W. Deng, and E. Barkai, Renewal theory with fat-tailed distributed sojourn times: Typical versus rare, Phys. Rev. E **98**, 042139 (2018).

[21] C. P. Dettmann, Diffusion in the Lorentz gas, Commun. Theor. Phys. **62**, 521 (2014).

[22] L. D'Alessio, Y. Kafri, A. Polkovnikov, and M. Rigol, From quantum chaos and eigenstate thermalization to statistical mechanics and thermodynamics, Adv. Phys. **65**, 239 (2016).

[23] A. Dubkov, A. Krasnova, and O. Chichigina, Influence of harmonic perturbation on speed of billiard particle, Fluct. Noise Lett. **18**, 1940012 (2019).

[24] O. A. Chichigina and D. Valenti, Strongly super-Poisson statistics replaced by a wide-pulse Poisson process: The billiard random generator, Chaos Solitons Fractals **153**, 111451 (2021).

[25] A. Nagar and S. Gupta, Diffusion with stochastic resetting at power-law times, Phys. Rev. E **93**, 060102(R) (2016).

[26] A. Pal, A. Kundu, and M. R. Evans, Diffusion under time-dependent resetting, J. Phys. A: Math. Theor. **49**, 225001 (2016).

[27] V. P. Shkilev, Continuous-time random walk under time-dependent resetting, Phys. Rev. E **96**, 012126 (2017).

[28] P. C. Bressloff, Queueing theory of search processes with stochastic resetting, Phys. Rev. E **102**, 032109 (2020).

[29] A. Iliopoulos, D. Chorozoglou, C. Kourouklas, O. Mangira, and E. Papadimitriou, Memory and renewal aging of strong earthquakes in Hellenic seismicity, Chaos Solitons Fractals **131**, 109511 (2020).

[30] S. Reich and R. Rosenbaum, The impact of short term synaptic depression and stochastic vesicle dynamics on neuronal variability, J. Comput. Neurosci. **35**, 39 (2013).

[31] O. A. Chichigina, Noise with memory as a model of lemming cycles, Eur. Phys. J. B **65**, 347 (2008).

[32] E. I. Anashkina, O. A. Chichigina, D. Valenti, A. V. Kargovsky, and B. Spagnolo, Predator population depending on lemming cycles, Intl. J. Mod. Phys. B **30**, 1541003 (2016).

[33] B. I. Camara, R. Yamapi, and H. Mokrani, How do copper contamination pulses shape the regime shifts of phytoplankton-zooplankton dynamics? Commun. Nonlinear Sci. Numer. Simulat. **48**, 170 (2017).

[34] M. Ogura, M. Wakaiki, H. Rubin, and V. M. Preciado, Delayed bet-hedging resilience strategies under environmental fluctuations, Phys. Rev. E **95**, 052404 (2017).

[35] O. A. Chichigina, A. V. Kargovsky, and D. Valenti, Role of sub- and super-Poisson noise sources in population dynamics, J. Stat. Mech. (2020) 093501.

[36] Y. Wu, Y. Jiao, Y. Zhao, H. Jia, and L. Xu, Noise-induced quasiperiod and period switching, Phys. Rev. E **105**, 014419 (2022).

[37] W. Whitt, Approximating a point process by a renewal process, I: Two basic methods, Oper. Res. **30**, 125 (1982).

[38] A. Pease, K. Mahmoodi, and B. J. West, Complexity measures of music, Chaos Solitons Fractals **108**, 82 (2018).

[39] X. Zhang, R. Ma, and L. Wang, Predicting turning point, duration and attack rate of COVID-19 outbreaks in major Western countries, Chaos Solitons Fractals **135**, 109829 (2020).

[40] B. Finkenstädt and B. Grenfell, Empirical determinants of measles metapopulation dynamics in England and Wales, Proc. R. Soc. London B **265**, 211 (1998).

[41] B. F. Finkenstädt and B. T. Grenfell, Time series modelling of childhood diseases: A dynamical systems approach, J. R. Stat. Soc. C **49**, 187 (2000).

[42] A. Ihler, J. Hutchins, and P. Smyth, Adaptive event detection with time-varying poisson processes, in *Proceedings of the 12th ACM SIGKDD International Conference on Knowledge Discovery and Data Mining*, edited by L. Ungar, M. Craven, D. Gunopulos, and T. Eliassi-Rad (ACM, New York, 2006), pp. 207–216.

[43] J. H. Myers, Synchrony in outbreaks of forest Lepidoptera: A possible example of the Moran effect, Ecology **79**, 1111 (1998).

[44] A. V. Kargovsky, E. I. Anashkina, O. A. Chichigina, and A. K. Krasnova, Velocity distribution for quasistable acceleration in the presence of multiplicative noise, Phys. Rev. E **87**, 042133 (2013).

[45] J. Demers and C. Jarzynski, Universal energy diffusion in a quivering billiard, Phys. Rev. E **92**, 042911 (2015).

[46] D. T. Hristopulos, B. Spagnolo, and D. Valenti, Open challenges in environmental data analysis and ecological complex systems, Europhys. Lett. **132**, 68001 (2020).

[47] B. R. Levin, *Theoretical Principles of Statistical Radiophysics* (Radio and Communications, Moscow, 1989).

[48] O. A. Chichigina, A. A. Dubkov, D. Valenti, and B. Spagnolo, Stability in a system subject to noise with regulated periodicity, Phys. Rev. E **84**, 021134 (2011).

[49] E. T. Whittaker and G. N. Watson, *A Course of Modern Analysis* (Cambridge University Press, Cambridge, 1996).

[50] P. D. Miller, *Applied Asymptotic Analysis* (American Mathematical Society, Providence, 2006).

[51] P. Lansky, L. Sacerdote, and C. Zucca, The Gamma renewal process as an output of the diffusion leaky integrate-and-fire neuronal model, Biol. Cybern. **110**, 193 (2016).

[52] R. F. Pawula, J. M. Porrà, and J. Masoliver, Mean first-passage times for systems driven by gamma and McFadden dichotomous noise, Phys. Rev. E **47**, 189 (1993).

[53] M. Matsumoto and T. Nishimura, Mersenne twister: A 623-dimensionally equidistributed uniform pseudo-random number generator, ACM Trans. Model. Comput. Simul. **8**, 3 (1998).

[54] V. V. Voevodin, A. S. Antonov, D. A. Nikitenko, P. A. Shvets, S. I. Sobolev, I. Y. Sidorov, K. S. Stefanov, V. V. Voevodin, and S. A. Zhumatiy, Supercomputer Lomonosov-2: Large scale, deep monitoring and fine analytics for the user community, Supercomp. Front. Innov. **6**, 4 (2019).

[55] A. Erdélyi, W. Magnus, F. Oberhettinger, and F. G. Tricomi, *Higher Transcendental Functions* (McGraw-Hill, New York, 1953).